doi.org/10.36721/PJPS/2026.40.16763.1

A silk fibroin-based dissolvable microneedle for transdermal delivery of scorpion venom protein

Xiaoyan Lu[1]*, Bo Li[1], Shoujuan Yang[1], Shiwang Fan[2], Mengqi Li[1], Shujun Shi[1], Hongbao Liang[1] and Yongchao Chu[2]*

[1]Department of Traditional Chinese Medicine, Shandong College of Traditional Chinese Medicine, Yantai, 264199, Shandong, People's Republic of China

[2]School of Pharmacy, Key Laboratory of Molecular Pharmacology and Drug Evaluation (Yantai University), Ministry of Education, Collaborative Innovation Center of Advanced Drug Delivery System and Biotech Drugs in Universities of Shandong, Yantai University, 30 Qingquan Road, Yantai, 264005, Shandong, People's Republic of China.

Abstract: **Background**: Scorpion venom protein (SVP) possesses potent analgesic activity but requires daily intramuscular injection, severely compromising patient compliance. Transdermal delivery offers a painless alternative, yet the stratum corneum limits macromolecular permeation. **Objectives**: This study aimed to develop a silk fibroin (SF)-based dissolvable microneedle patch for transdermal delivery of SVP, enabling prolonged analgesic effect following a single administration. **Methods**: Dissolvable microneedles were fabricated using SF as a sustained-release matrix for needle tips and polyacrylic acid (PAA) as a soluble backing layer. Microneedles were characterized for morphology, mechanical strength, skin penetration ability and backing dissolution time. Skin irritation was assessed in male Sprague-Dawley (SD) rats. Analgesic efficacy was evaluated in male BALB/c mice using acetic acid-induced writhing and tail-flick assays, comparing the microneedle patch with intramuscular injection. **Results**: The fabricated microneedles were conical, ~590 μm in length, enabling effective penetration of mouse skin. The PAA backing dissolved completely within 5 min in phosphate-buffered saline (PBS). No skin irritation (erythema or edema) was observed. In the writhing test, the microneedle group showed inhibition rates of 74.0% at 1 h and 72.4% at 4 h; by contrast, the injection group showed 69.1% at 1 h but dropped sharply to 8.0% at 4 h. The tail-flick assay confirmed prolonged analgesia with microneedle application. **Conclusion**: SVP-loaded SF-based dissolvable microneedles are safe, provide sustained analgesic effects and represent a promising alternative to frequent injections for chronic pain management.

Keywords: Dissolvable microneedle; Scorpion venom protein; Silk fibroin; Sustained analgesia; Transdermal delivery

Submitted 12-05-2026 – Revised 29-08-2026 – Accepted 03-09-2026

INTRODUCTION

SVP, the primary active component of Chinese medicine scorpion venom injection, has significant, broad-spectrum analgesic activity. Scorpion venom injection is an approved proprietary Chinese medicine manufactured by Tonghua Weijing Pharmaceutical Co., Ltd. It is currently used clinically to relieve mild-to-moderate pain associated with conditions such as scapulohumeral periarthritis, osteoarthritis, and rheumatoid arthritis. Mechanistic studies suggest that its analgesic effects involve modulating voltage-gated sodium channels, suppressing inflammatory cytokine release, and activating descending inhibitory pathways (Mao *et al*., 2013; Mosaddeghi-Heris *et al*., 2026). Despite these therapeutic benefits, the current formulation suffers from severe administration-related drawbacks. Each ampoule (1 mL) contains 10 or 20 μg of protein and requires intramuscular injection into the gluteal muscle once or twice daily. For patients with chronic pain requiring long-term, sustained medication, such frequent invasive injections not only cause injection-site pain and tissue damage but also drastically reduce patient compliance, sometimes forcing treatment discontinuation (Wei *et al*., 2025). Thus, developing a painless, safe and long-acting delivery method for SVP is a key scientific question to maximize its clinical potential.

Transdermal drug delivery systems (TDDS) are an excellent alternative for parenteral administration. By delivering drugs through the skin, TDDS bypass gastrointestinal degradation and hepatic first-pass metabolism, extend dosing intervals, reduce fluctuations in plasma drug concentrations and minimize systemic side effects (Meng *et al*., 2016). Compared with injections, TDDS are painless, self-administrable, convenient and safe. However, the stratum corneum acts as a formidable physical barrier that severely limits percutaneous drug penetration, particularly for macromolecules. (Gupta *et al*., 2021) To date, approximately 33 transdermal formulations have been approved worldwide, all with molecular weights below 500 Da, highlighting a fundamental limitation of conventional TDDS for macromolecular delivery (Ghosh *et al*., 2026; Wei *et al*., 2025; Zhang *et al*., 2024). Recent advances in biomaterials and drug delivery technologies have expanded the therapeutic applications of peptide and protein drugs (Liu *et al*., 2024; Wang *et al*., 2022; Wang *et*

**Corresponding author:* e-mail: ytuyongchao@163.com; luxiaoyan@sdctcm.edu.cn

al., 2025; Xiao *et al*., 2025; Zeng *et al*., 2025; Zheng *et al*., 2025). Microneedles, ranging from 25 to 2,000 μm in length, can penetrate the stratum corneum to create micron-sized channels, dramatically enhancing skin permeability to drugs, including macromolecules, while avoiding dermal pain receptors for painless administration (Cheung *et al*., 2015; Van Damme *et al*., 2009). Among microneedle types, dissolvable microneedles, fabricated by mixing polymers with drugs, offer advantages including biodegradability, high drug-loading capacity, and the absence of sharp waste residues (Moawad *et al*., 2025). However, synthetic polymers are often hydrophobic, and their degradation products tend to induce local inflammatory responses, limiting their applicability (Wu *et al*., 2024). Therefore, developing natural polymers with excellent biocompatibility, biodegradability and sustained-release functionality has become a key focus of dissolvable microneedle research.

SF is an amphiphilic natural protein whose ordered hydrophobic domains form strong antiparallel β-sheets, endowing it with excellent mechanical strength (Huang *et al*., 2018; Lin *et al*., 2025). Because of its superior biocompatibility, biodegradability, aqueous-based processability, tunable structure and properties, and stabilizing effects on biological macromolecules, SF has been extensively explored for various drug delivery systems, including nanoparticles, hydrogels, implants, and microneedles (Li *et al*., 2015; Wang *et al*., 2024). Given its outstanding sustained-release performance and mechanical strength, SF is an ideal polymeric material for constructing sustained-release dissolvable microneedles. In light of this, a novel sustained-release dissolvable microneedle was designed using SF as the sustained-release matrix for the needle tips and water-soluble PAA as the backing layer for transdermal delivery of SVP. Upon skin insertion, the PAA backing rapidly dissolves, allowing the drug-loaded SF tips to separate from the backing and remain embedded in the skin. Subsequently, the SF tips degrade slowly, achieving sustained SVP release and thereby producing long-lasting analgesia. This delivery strategy has the potential to fundamentally transform the current paradigm of daily SVP injections, enabling a painless, once-per-administration treatment modality. It offers a novel solution for treating chronic inflammatory diseases such as rheumatoid arthritis and has significant potential for clinical translation.

BALB/c mice were used for the writhing and tail-flick tests to assess peripheral and central analgesia, respectively (Mao *et al*., 2013; Bezerra *et al*., 2023; Zhu *et al*., 2022), while SD rats were used for the skin irritation test because their dorsal skin is suitable for standardized patch application and Draize scoring (Oshizaka *et al*., 2023). It was hypothesized that SVP-loaded SF dissolvable microneedles would provide early analgesic efficacy comparable to intramuscular injection and more sustained subsequent analgesia, without causing skin irritation.

MATERIALS AND METHODS

Materials

SVP was purchased from Shijiazhuang Xietaitai Biotechnology Co., Ltd. SF was purchased from Simatech (Suzhou, China). PAA were sourced from Millipore Sigma (Burlington, MA). BeyoBCA peptide assay kit was purchased from Beyotime Biotechnology Co., Ltd. Polydimethylsiloxane (PDMS) mold purchased from Guangzhou Shiling Laike Mold Commercial Firm.

Animals

Male BALB/c mice (6–8 weeks old) and male SD rats (6–8 weeks old) (specific pathogen-free) were supplied by Yantai Yide Experimental Animal Breeding Co. LTD. Mice were used for the writhing, tail-flick, and skin insertion tests; rats were used for the skin irritation test. Animals were housed at 22 ± 2 °C on a 12 h light/dark cycle with free access to food and water and nesting material. After 7 days of acclimatization, humane endpoints (>20% weight loss, severe lethargy, or persistent self-mutilation) were applied, and no adverse events were observed during the study. All animals were euthanized with an overdose of pentobarbital sodium via intraperitoneal injection at the end of the study.

Preparation of SVP microneedles

Lyophilized SF powder (50 mg) was dissolved in 1 mL of deionized water and allowed to swell for 30 min at room temperature. Subsequently, 20 mg of SVP lyophilized powder was added to the swollen SF solution and the mixture was stirred at 400 rpm for 30 min at room temperature using a magnetic stirrer to obtain a homogeneous solution (NMS6Pro, Qun'an Scientific Instruments Co., Ltd.). The resulting mixture was then pipetted into a 10 × 10 PDMS mold (needle length: 600 μm, base diameter: 300 μm, tip-to-tip spacing: 600 μm). The mold was centrifuged in a horizontal rotor centrifuge at 2,800 rpm at 10 °C (LD5-2A, Beijing Medical Centrifuge Factory). Excess liquid was removed from the mold, which was then placed in an incubator for 20 h to allow the needle tips to form. The mold was subsequently transferred to a desiccator containing 500 mL methanol at the bottom and incubated at room temperature for 48 h. PAA was added using a positive-displacement pipette, followed by another centrifugation step at 2,800 rpm at 10 °C (LD5-2A, Beijing Medical Centrifuge Factory). The mold containing the composite microneedles was dried in a desiccator for 72 h, after which the microneedles were demolded and stored in a desiccator (307mm, Hunan Xiangbo Glass Co., Ltd.).

Morphology and structure

The morphology of the microneedles was examined using a stereomicroscope with a cold light source (SZMN7045TR, Sunny Optical Technology Co., Ltd) and images were captured to assess microneedle integrity. The

In Press

Table 1: Formulation composition of SVP-loaded dissolvable microneedle patch

Component	SVP	SF	PAA	Deionized water
Amount per patch	20 mg	50 mg	150μL	1mL

microstructure of the microneedles was further observed using scanning electron microscopy (SEM) (MVE048594, Funa Scientific Instruments Co., Ltd) (Qi *et al*., 2023).

Secondary structure characterization

Microneedles were ground with dried KBr under an infrared lamp to a particle size of less than 200 mesh. The mixture was compressed into a pellet and fourier-transform infrared (FTIR) spectra were recorded with automatic atmospheric background subtraction (Nicolet iS 5, Thermo Fisher Scientific) (Yin *et al*., 2018).

Mechanical properties

Microneedle arrays were placed on the test stage of a texture analyzer (Universal TA, Shanghai Tengji Instrument Technology Co., Ltd). A P/5 probe was used to measure the fracture force of individual microneedle tips (Zhu *et al*., 2020). The probe moved vertically toward the microneedle tip at a speed of 0.1 mm/s. The probe traveled 0.5 mm from the microneedle tip toward the patch backing and the fracture force was recorded.

Skin insertion ability

Excised mouse skin was cleaned and flattened. A microneedle patch was pressed into the skin for 10 s and then removed it. The insertion sites were stained with methylene blue and examined the skin under a microscope (SZMN7045TR, Sunny Optical Technology Co., Ltd.). In addition, treated skin samples were excised, fixed in 4% paraformaldehyde, embedded in paraffin, sectioned, and stained with hematoxylin and eosin (H&E) to observe microneedle penetration depth under a microscope (CX33, Olympus Corporation) (Jiang *et al*., 2026).

Parafilm insertion test

Parafilm M® (PF) film with a thickness of approximately 126 μm serves as a convenient *in-vitro* model for microneedle skin insertion testing (Larraneta *et al*., 2014). Microneedles were pressed onto 10 layers of PF film with approximately 70 N of force. The number of needles penetrating each layer was recorded. The test was performed in triplicate. The penetration rate was calculated as follows:

Penetration rate (%) = (Number of needles penetrating each layer / Total number of needles per patch) × 100%

Backing separation performance

Microneedle arrays were adhered to the bottom of a 12-well plate and PBS (pH 7.4) was added. The plate was placed in a constant-temperature incubator (DHG-9245A, Shanghai Yiheng Scientific Instruments Co., Ltd.) at 37 ± 2 °C. The separation of the SF needle tips from the PAA backing was monitored under a stereomicroscope at 0 min, 1 min, 3 min, 5min and the time required for complete separation was recorded (Lu *et al*., 2022).

Degradation behavior

The biodegradability of the microneedles was evaluated using an *in vitro enzymatic degradation assay* (Lu *et al*., 2022). Microneedles were immersed in PBS (pH 7.4) containing protease XIV (2 U/mL). Microneedles immersed in PBS (pH 7.4) without the enzyme served as controls. Images were taken on days 0, 1, 2, 4, 6 and 8 (SZMN7045TR, Sunny Optical Technology Co., Ltd.).

Skin irritation

Skin irritation was evaluated using the Draize method (Oshizaka *et al*., 2023). The dorsal hair of rats was shaved. The dorsal hair of SD rats (male, 6–8 weeks old, weighing approximately 200 g) was shaved. The rat was anesthetized by inhalation of isoflurane (5% for induction, 2–3% for maintenance, in 100% oxygen at a flow rate of 1 L/min) using a laboratory animal anesthesia machine (ABS-4A, Shanghai Yuyan Scientific Instrument Co., Ltd.). After anesthesia was confirmed, microneedles were inserted into the dorsal skin with manual compression for 3 min. After removal of the microneedle backing, the skin was photographed (SZMN7045TR, Sunny Optical Technology Co., Ltd.). Erythema and edema were recorded before administration (0 h, baseline control) and at 1 and 3 h post-administration.

In-vitro release study

Fluorescein isothiocyanate (FITC)-labeled SVP (FITC-SVP) was prepared for *in-vitro* release studies (Lantz *et al*., 2023). Briefly, 5 mg of SVP was dissolved in 2.5 mL of carbonate-bicarbonate buffer (pH 9.0). FITC was dissolved in dimethylsulfoxide (DMSO) at a concentration of 1 mg/mL. Under magnetic stirring at 400 rpm (NMS6Pro, Qun'an Scientific Instruments Co., Ltd.), 250 μL of the FITC/DMSO solution was slowly added to the SVP buffer solution in multiple portions. The mixture was allowed to react at room temperature in the dark for 3 h. After the reaction, the mixture was transferred to an ultrafiltration tube (MWCO 10kDa, Millipore) and centrifuged at 4,000 rpm for 15 min at 4 °C. The retentate was collected as FITC-SVP and stored at 4 °C until use. The FITC-SVP was then used to prepare microneedles following the same procedure described in section 2.2.

For the *in-vitro* release study, the prepared FITC-SVP-loaded microneedles were placed in a centrifuge tube containing 5 mL of PBS (pH 7.4) and incubated at 37 °C in a constant-temperature shaking incubator (DKZ-1,

Shanghai Yiheng Scientific Instruments Co., Ltd.) (Li *et al*., 2025). At predetermined time points (2, 6, 8, 12 and 24 h), 1 mL of the release medium was withdrawn and replaced with an equal volume of fresh PBS. The fluorescence intensity of the collected samples was measured using a fluorescence spectrophotometer (F-320, Tianjin Gangdong Technology Co., Ltd) and the cumulative release percentage was calculated. All release measurements were performed in triplicate.

Acetic acid-induced writhing test

The acetic acid-induced writhing test was performed according to a previously reported method (Bezerra *et al*., 2023). Fifteen BALB/c mice (6–8 weeks old) were randomly divided into three groups by simple random assignment (n = 5 per group): saline control, SVP injection and SVP-loaded microneedle groups. For the injection group, each mouse received 10 μg of SVP via tail vein injection. For the microneedle group, an SVP-loaded microneedle patch was applied to the shaved abdominal skin and held in place with gentle manual compression for 3 min to ensure complete insertion. At 1 h and 4 h post-administration, each mouse was intraperitoneally injected with 0.6% acetic acid solution at a dose of 10 mL/kg. The number of writhes was recorded over a 15 min period. The writhing inhibition rate was calculated as:

Inhibition rate (%) = [(Writhing count in control group – Writhing count in treatment group) / Writhing count in control group] × 100%

Tail-flick test

The tail-flick test was conducted following previously established protocols (Zhu *et al*., 2022). Fifteen BALB/c mice (6–8 weeks old) were randomly divided into three groups (n = 5 per group): saline control, SVP injection and SVP-loaded microneedle groups. For the injection group, each mouse received 10 μg of SVP via tail vein injection. For the microneedle group, mice were manually restrained in the prone position. An SVP-loaded microneedle patch was applied to the shaved abdominal skin and held it in place with gentle manual compression for 3 min to ensure complete insertion. At 1 h and 4 h post-administration, the distal 3 cm of the mouse tail was immersed in a constant-temperature water bath maintained at 50 °C (TWS-26, Shanghai Zhetu Scientific Instrument Co., Ltd.). The tail-flick latency, defined as the time from tail immersion to the first rapid flick of the tail, was measured using a stopwatch. The maximum immersion time was set to 10 s to prevent tissue damage.

Statistical analysis

Statistical analyses were conducted using GraphPad Prism 10 (San Diego, CA, U.S.A.). Between group differences were compared using two-way ANOVA with an unpaired t-test. A value of $P < 0.05$ was considered statistically significant.

RESULTS

Microneedle fabrication and characterization

Each patch contained approximately 1.178 μL of drug solution in total, corresponding to a theoretical SVP loading of 23.56 μg per patch based on the formulation concentration (for calculation details, see Supplementary Materials). Stereomicroscopy revealed that the fabricated microneedles had a conical shape, uniform distribution, and intact morphology (Fig. 1A–C). The needles measured approximately 590 μm in length and 295 μm in base diameter. SEM images showed a wrinkled surface texture and a dense overall structure without apparent collapse (Fig. 1D–F and Fig. S1).

FTIR spectroscopy

The FTIR spectrum of SF is characterized by a series of amide absorption bands, among which the amide I region (1,600–1,700 cm^{-1}) is a key feature. As shown in Fig. 2 and Fig. S2, the amide I peak of raw SF was located at 1,658 cm^{-1} and the amide II peak at 1,533 cm^{-1}, indicating that SF predominantly adopted a random coil/α-helical conformation. After microneedle fabrication, the amide I peak of blank SF microneedles shifted slightly to 1,655 cm^{-1}, suggesting a partial transition to β-sheet structures. Upon SVP loading, the amide I peak further red-shifted to 1,629 cm^{-1} and the amide II peak shifted to 1,528 cm^{-1}, demonstrating that the incorporation of SVP significantly induced β-sheet formation in SF.

In-vitro skin penetration and insertion performance

A PF film approximately 126 μm thick serves as a convenient in *vitro* model for microneedle skin insertion testing (Larraneta *et al*., 2014). As shown in Fig. 3A and B, the microneedle tips successfully penetrated the first and second PF layers, with a penetration rate exceeding 95% for the third layer. However, the penetration rate dropped sharply to below 10% for the fourth layer and no penetration was observed for the fifth or sixth layers. The SF microneedles penetrated to a depth of approximately 378 μm (equivalent to three PF layers). Owing to the elasticity and toughness of PF, which resemble those of skin, the actual penetration depth was less than the needle length.

Skin insertion tests confirmed successful penetration into excised mouse skin, generating uniform microchannels (Fig. 3C and Fig. S3). The fracture force of SVP-loaded microneedles was 13.84 N (Fig. 3D). Optical microscopy images showed the morphology of microneedles before and after compression using a texture analyzer. After compression, slight tip deformation was observed at the needle tips, while the needle shafts remained intact (Fig. S4). H&E staining of treated skin sections further confirmed that the microneedles penetrated the stratum corneum and epidermis, with microchannels reaching the superficial dermis. The measured penetration depth exceeded 200 μm (Fig. S5).

In Press

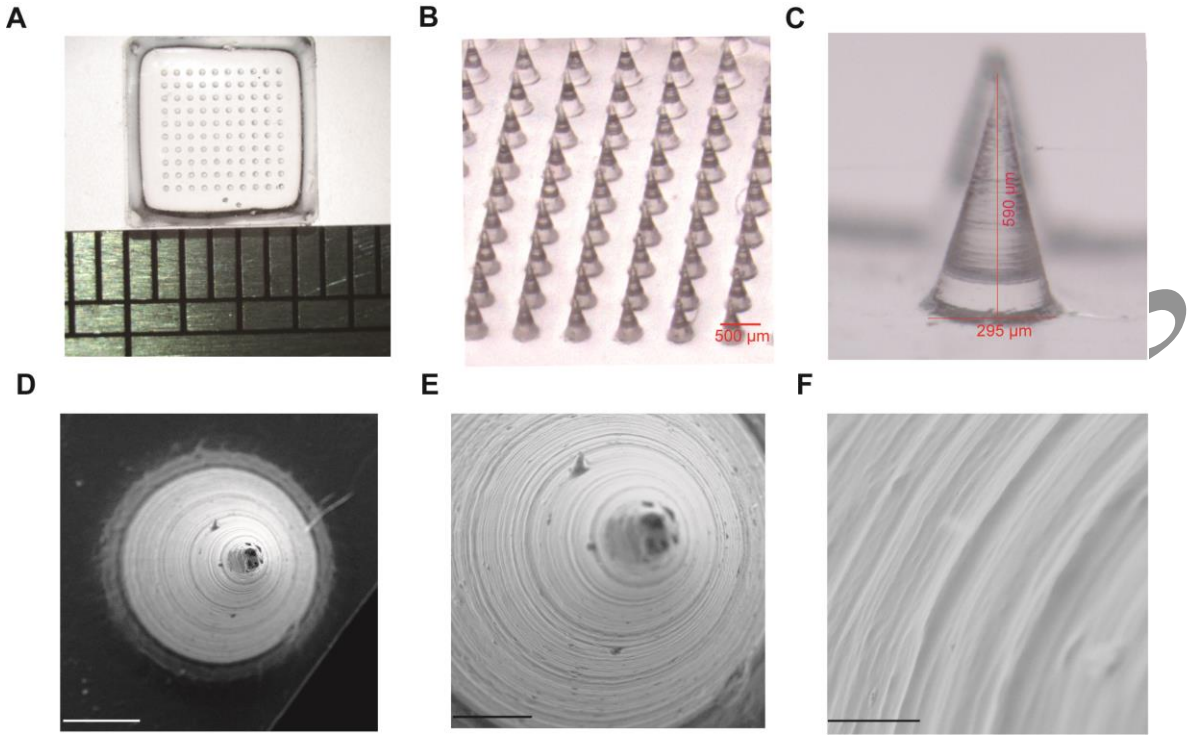


Fig. 1: Morphology of SVP-loaded microneedles. (A) Stereomicroscopic image showing microneedle dimensions; a ruler with 1 mm divisions is shown for size reference. (B) Side-view stereomicroscopic image of microneedles. Scale bars: 500 µm; (C) Stereomicroscopic image of single microneedle; (D–F) SEM images at different magnifications. Scale bars: 100 µm (D), 50 µm (E), and 8 µm (F).

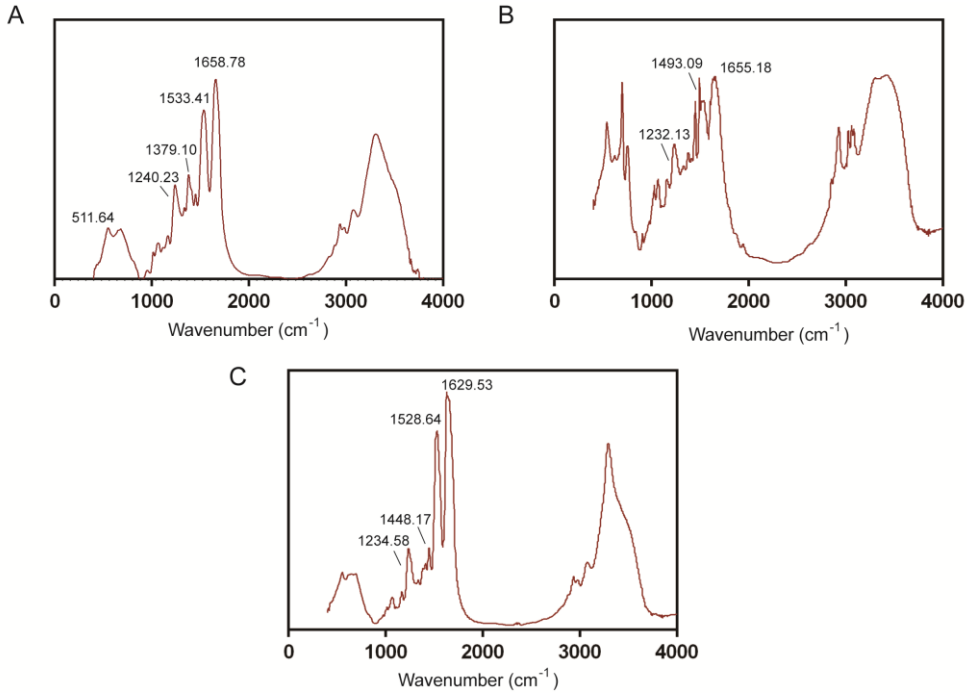


Fig. 2: FTIR spectra (A) Raw SF; (B) Blank SF microneedles; (C) SVP-loaded SF microneedles.

Backing separation and degradation behavior

To determine whether the PAA backing rapidly separates from the SF needle tips upon contact with tissue fluid, a separation test was performed in PBS. The PAA backing dissolved within 5 min, allowing the needle tips to detach from the backing. Complete separation of all needle tips from the backing occurred within approximately 5 min (Fig. 4A). Degradation experiments showed that on day 1, the

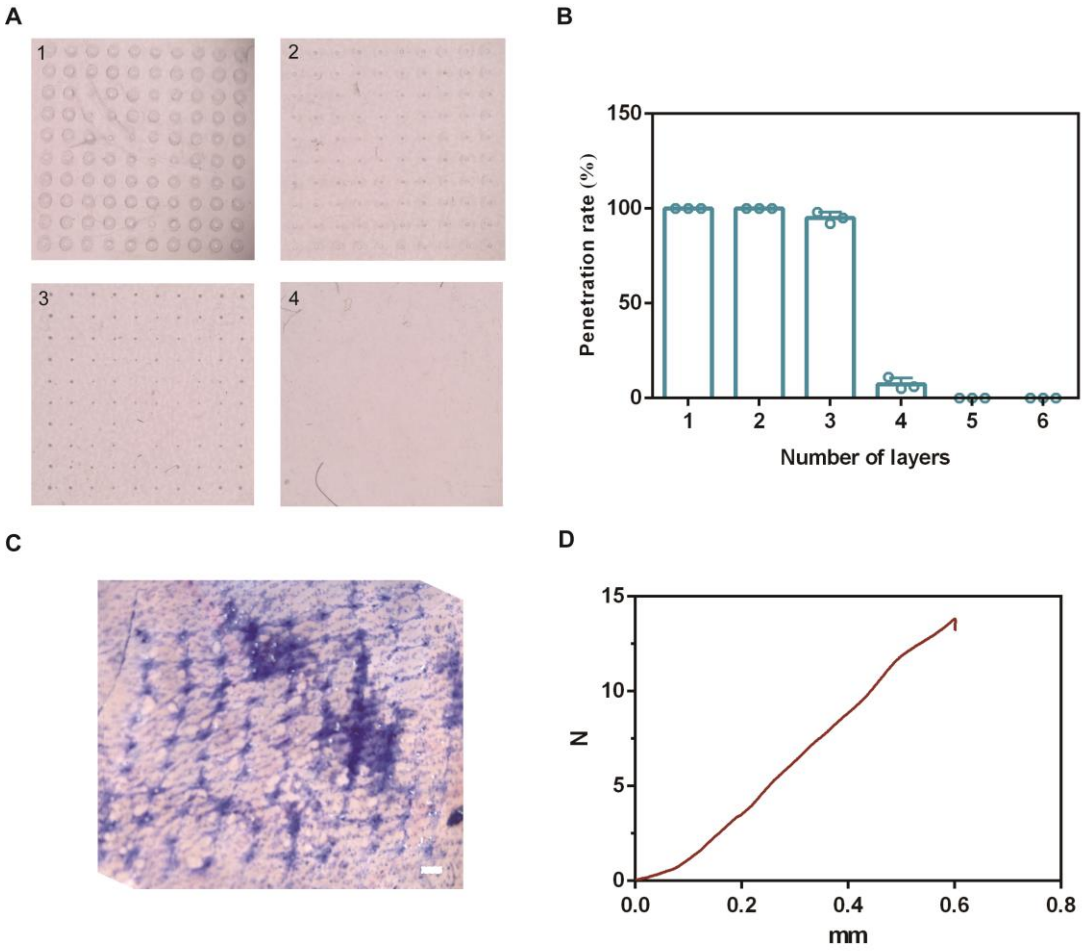


Fig. 3: Penetration performance. (A) Parafilm insertion test; (B) Penetration rate as a function of Parafilm layer (mean ± SD, n = 3). Each dot represents one independent measurement); (C) Skin insertion of SVP-loaded microneedles into excised mouse skin, Scale bars: 500 μm; (D) Mechanical properties showing fracture force.

PAA backing had dissolved in both PBS and protease XIV solution and the needle tips began to separate. Over time, the needle tips gradually degraded in protease XIV solution, with most of the tips degraded by day 8. In contrast, no substantial degradation was observed in PBS (pH 7.4) during the first four days, with only a slight reduction by day 8 (Fig. 4B).

Skin irritation

As shown in Fig. 5, upon removal of the microneedle patch, the skin surface exhibited visible needle puncture marks but no erythema, swelling, or edema. These marks had largely disappeared by 3 h post-administration, indicating minimal skin irritation.

In-vitro release study

The *in vitro* release profile of FITC-labeled SVP from the SF microneedles showed sustained release behavior (Fig. 6). At 2 h and 6 h, the cumulative release rates were 36.8% and 44.0%, respectively, indicating relatively slow release during the initial 6 h. The release rate then increased markedly, reaching 77.1% at 8 h and 96.6% at 12 h, suggesting that most SVP was released within 12 h.

In-vivo analgesic efficacy

In the writhing test (Fig. 7A; Table 2), the microneedle group achieved a writhing inhibition rate of 74.0% at 1 h post-administration, comparable to that of the SVP injection group (69.1%). At 4 h, the microneedle group maintained a high inhibition rate of 72.4%, whereas the injection group's inhibition rate dropped sharply to 8.0% ($p < 0.01$).

In the tail-flick test (Fig. 7B), the microneedle group exhibited a tail-flick latency of 5.67 s at 1 h, compared with 4.19 s for the injection group and 1.88 s for the saline control group ($p < 0.05$). At 4 h, the microneedle group still showed a latency of 3.91 s, which remained higher than that of the injection group (2.47 s, $p < 0.05$) and the saline control (1.88 s, $p < 0.05$).

DISCUSSION

In this study, a silk fibroin-based dissolving microneedle patch was developed for transdermal delivery of scorpion venom protein as a sustained-release alternative to daily

Article

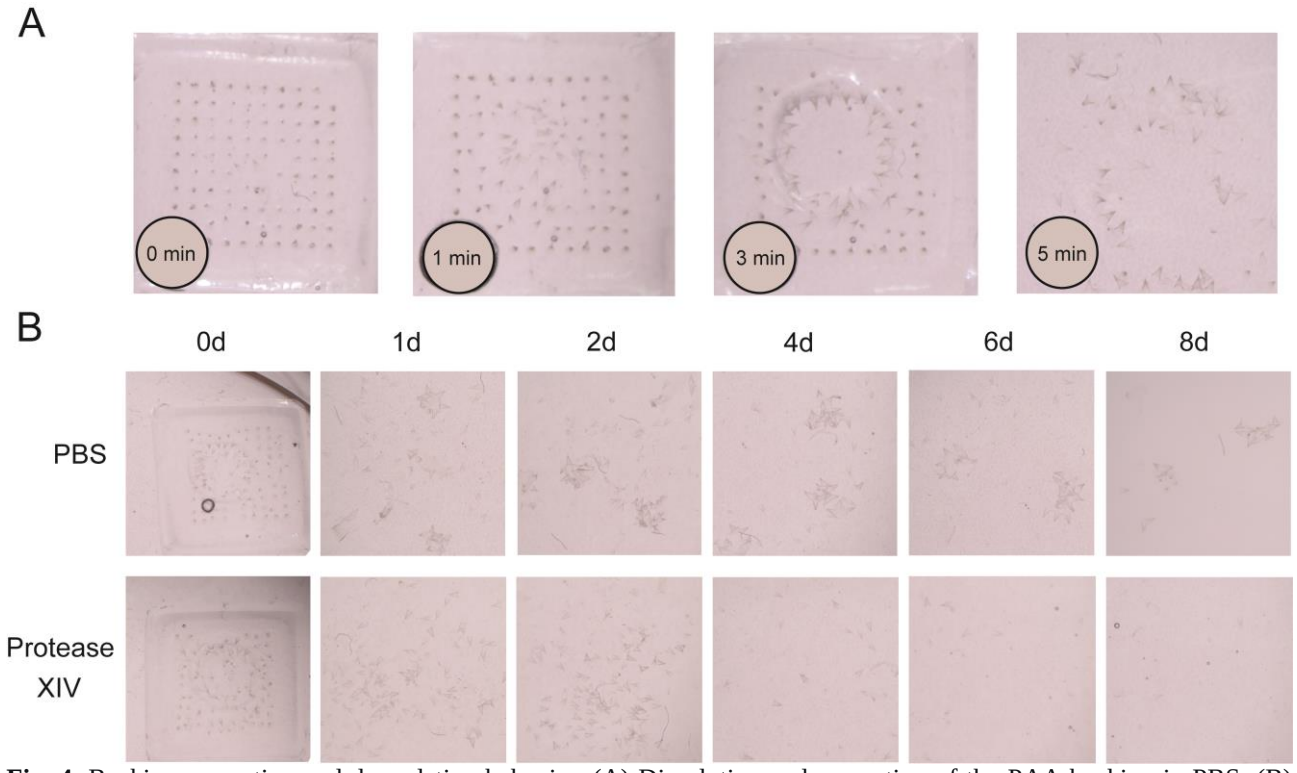


Fig. 4: Backing separation and degradation behavior. (A) Dissolution and separation of the PAA backing in PBS; (B) Degradation of microneedles in PBS and protease XIV solution over 8 days.

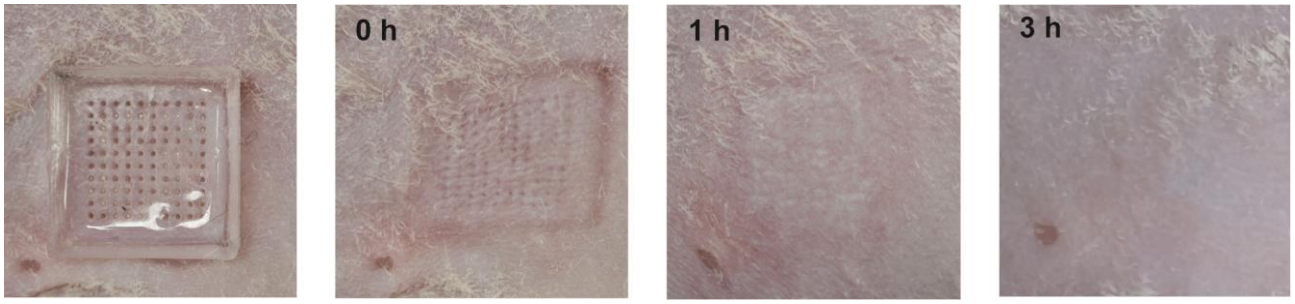


Fig. 5: Representative images of rat skin before and after microneedle administration.

intramuscular injections. The fabricated microneedles exhibited uniform conical morphology with a length of approximately 590 μm and a base diameter of 295 μm (Fig. 1), comparable to previously reported SF-based microneedle systems (Lu *et al*., 2022). Each microneedle patch contained approximately 23 μg of SVP, which is comparable to the daily dose of the commercially available scorpion venom injection. In the FTIR analysis, the conformational rearrangement of SF from random coil/α-helix to β-sheet upon SVP loading is likely attributable to strong hydrogen bonding or electrostatic interactions between SVP and SF molecules.

The fracture force of 13.84 N (Fig. 3D) exceeded the 10 N threshold considered sufficient for skin insertion(Larrañeta *et al*., 2014). The Parafilm test demonstrated penetration through three layers (approximately 378 μm), exceeding the combined thickness of human stratum corneum and epidermis (approximately 300 μm). Skin insertion tests using excised mouse skin confirmed successful penetration, as shown by methylene blue staining (Fig. 3C) and H&E staining of skin cross-sections (Fig. S5), with microchannels extending beyond 200 μm into the dermis. These findings are consistent with previous microneedle insertion studies (Qi *et al*., 2023; Wang *et al*., 2024).

The PAA backing dissolved completely within 5 min in PBS (Fig. 4A), enabling rapid separation of the SF tips from the backing upon skin application, comparable to other rapidly separable microneedle systems (Lu *et al*., 2022). The SF tips gradually degraded in protease XIV solution, with most tips degraded by day 8. In contrast, PBS without enzyme showed minimal degradation (Fig. 4B). This enzyme-dependent degradation is consistent with the known biodegradability of SF (Li *et al*., 2025).

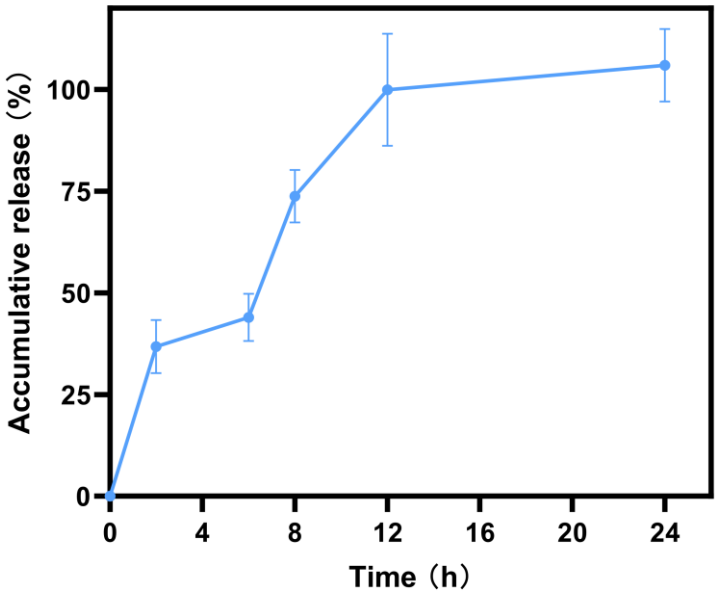


Fig. 6: *In-vitro* cumulative release profile of FITC-labeled SVP from SF-based dissolving microneedles in PBS (pH 7.4). Data are presented as mean ± SD (n = 3).

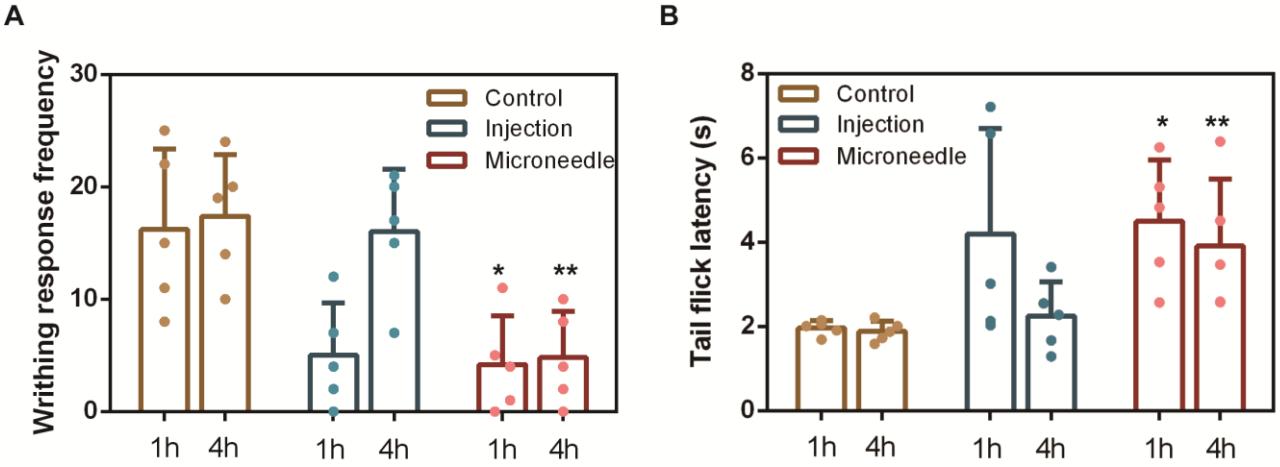


Fig. 7: *In vivo* analgesic efficacy. (A) Acetic acid-induced writhing test; (B) Tail-flick test. (mean ± SD, n = 5). (A) **p* = 0.0127, ***p* = 0.0034 vs. saline. (B) ***p* = 0.0048, **p* = 0.0232 vs. saline.

Table 2: Effect of SVP-loaded microneedles on acetic acid-induced writhing response in mice.

Group	Injection	Microneedle
Twist inhibition rate (1h)	69.1%	74.0%
Twist inhibition rate (4h)	8.0%	72.4%

The skin irritation study showed that visible puncture marks resolved within 3 h without erythema or edema (Fig. 5). Compared with chemical permeation enhancers and liposomal formulations, The microneedle system offers several advantages. Chemical enhancers often provide insufficient enhancement for macromolecules and may cause skin irritation at effective concentrations (Kovacik *et al.*, 2020). Liposomal systems require extensive formulation optimization for each payload and face stability challenges during storage (Saeidi *et al.*, 2023). In contrast, microneedle systems create a physical pathway across the stratum corneum regardless of molecular weight, avoid the irritancy and stability issues associated with other strategies, and involve a simpler fabrication process that may facilitate scale-up.

The *in vitro release study showed that the SF matrix provides sustained release of SVP, with most* SVP released

within 12 h and no significant burst release observed. The initial lag phase was attributed to the time required for SF matrix hydration (Li *et al*., 2025).

The *in vivo* analgesic efficacy of the SVP-loaded microneedles was evaluated using two complementary pain models: the acetic acid-induced writhing test and the tail-flick test. In the writhing test, the microneedle group achieved a 74.0% inhibition rate at 1 h, comparable to the injection group (69.1%), confirming that SVP delivered via microneedles retained its analgesic activity after fabrication. At 4 h post-administration, the microneedle group maintained a high inhibition rate of 72.4%, whereas the injection group showed a sharp decline to 8.0%. This marked difference in analgesic duration can be attributed to sustained SVP release from the SF matrix, which maintains therapeutic concentrations in the skin over time. In contrast, the injected SVP is rapidly cleared from the circulation, resulting in a short duration of action. These findings suggest that sustained release from the polymer matrix extends the therapeutic window compared to a single high-dose bolus injection.

In the tail-flick test, the microneedle group consistently showed longer latencies than the injection group at both 1 h and 4 h (Fig. 7B), further confirming the prolonged analgesic effect. The tail-flick test measures central pain responses, while the writhing test primarily reflects peripheral pain mechanisms. The consistency of results across both models suggests that the enhanced analgesic duration observed with microneedle delivery likely reflects a genuine pharmacokinetic/pharmacodynamic improvement.

The observation that the microneedle group maintained significant analgesia at 4 h, while the injection group had largely lost its effect, has important clinical implications. For patients with chronic pain conditions such as rheumatoid arthritis or osteoarthritis, who require long-term daily medication, the current injection regimen (once or twice daily) poses significant challenges in terms of patient compliance and quality of life (Deodhar *et al*., 2026; Tan *et al*., 2023). The microneedle system, with its prolonged action after a single application, offers the potential for less frequent dosing and improved patient adherence (Lu *et al*., 2022). This advantage is particularly relevant for chronic conditions where treatment discontinuation due to injection-related discomfort is a recognized clinical problem (Wei *et al*., 2025).

The development of innovative biomaterials and advanced manufacturing technologies has provided useful reference for the design and evaluation of microneedle-based protein delivery systems and these technological advances collectively support the continued refinement of transdermal delivery platforms for macromolecular therapeutics (Hu *et al*., 2024; Ng *et al*., 2024; Su *et al*., 2025; Yang *et al*., 2025). However, several limitations of this study should be acknowledged. First, the analgesic evaluation was limited to 1 h and 4 h post-administration, leaving the duration of action beyond 4 h unknown. Second, the *in vitro* release profile was determined using FITC-labeled SVP rather than unlabeled SVP because separating SVP from SF degradation products in the release medium is difficult. Third, systematic pharmacokinetic studies have not been, and the molecular mechanisms underlying the analgesic effect remain unexplored. Fourth, the present study was limited to single-dose administration in mice; the safety and efficacy of repeated dosing, including potential skin reactions with multiple applications, systemic accumulation, and maintenance of analgesic effect over extended periods, have not been evaluated. Fifth, the storage stability of the final product has not been systematically investigated; although the patches were stored in a desiccator at room temperature in the dark to minimize moisture uptake, long-term stability under different temperature and humidity conditions, shelf life, and retention of SVP bioactivity during storage remain to be characterized. Finally, species differences between rodent and human skin may affect the translational relevance of these findings. Future studies will address these limitations through extended observation windows, pharmacokinetic evaluations, mechanistic investigations, repeated-dose safety assessments and systematic stability studies according to relevant pharmaceutical guidelines.

Within the scope of this study, these findings suggest that the SVP-loaded SF microneedle patch is a safe, sustained-release transdermal formulation with potential for further investigation as an alternative to frequent injections for pain management.

CONCLUSION

In summary, a SF-based dissolvable microneedle patch was developed for transdermal delivery of SVP. The fabricated microneedles are uniform and conical, with adequate mechanical strength and effective skin penetration. The PAA backing dissolves within 5 min, allowing the sustained-release SF tips to remain in the skin, where they gradually degrade over 8 days *in-vitro*. *In vivo* evaluation in mouse pain models showed that the SVP-loaded microneedles achieved analgesic efficacy at 1 h comparable to conventional SVP injection. Importantly, at 4 h post-administration, the microneedle group maintained a robust analgesic effect, whereas the injection group showed a marked loss of efficacy. Moreover, we observed no skin irritation after microneedle application. These findings show that the SVP-loaded SF microneedle patch offers a patient-friendly, sustained-release alternative to daily injections, with strong potential to improve compliance and quality of life in patients requiring long-term pain management.

Supporting Information Available

Supplementary data associated with this article can be found in the online version, including the calculation of drug loading and Fig. S1–S5.

List of Abbreviations

DMSO, dimethyl sulfoxide; FITC, fluorescein isothiocyanate; FTIR, Fourier-transform infrared; H&E, hematoxylin and eosin; MWCO, molecular weight cut-off; PAA, polyacrylic acid; PBS, phosphate-buffered saline; PDMS, polydimethylsiloxane; PF, Parafilm; SD, Sprague–Dawley; SD, standard deviation; SEM, scanning electron microscopy; SF, silk fibroin; SVP, scorpion venom protein; TDDS, transdermal drug delivery systems.

Acknowledgements

The authors used DeepSeek for writing assistance and Nano Banana for the preparation of graphical abstract. All authors take full responsibility for the accuracy, originality and integrity of the content.

Authors' contributions

Xiaoyan Lu and Yongchao Chu designed the study and drafted the manuscript. Bo Li, Shoujuan Yang and Shiwang Fan performed experiments and collected data. Mengqi Li, Hongbao Liang and Shujun Shi analyzed data.

Funding

This study was supported by the Science and Technology Co-construction Project, Department of Science and Technology, State Administration of Traditional Chinese Medicine (GZY-KJS-SD-2024-052), Shandong Provincial Natural Science Foundation (ZR2023QH245) and Yantai Municipal University-Local Integration and Development Program (No. 2023XDRHXMXK07).

Data availability statement

The datasets generated during and/or analysed during the current study are available from the corresponding author on reasonable request.

Ethical approval

All animal studies were conducted in compliance with the protocols approved by the Animal Ethics Committee of Yantai University (Approval No. YTU20251201). The protocol was not registered in a public registry. This study was performed in adherence with the ARRIVE guidelines. See supplementary file for the ARRIVE checklist.

Consent to publication

Not applicable. This study did not involve human participants, and therefore informed consent for publication was not required. The funders had no role in the study design, data collection, analysis, interpretation, or preparation of the manuscript.

Conflict of interest

The authors have no competing interests.

REFERENCES

Bezerra LFG, Silva APSA, Cunha RXD, de Oliveira JRS, de Barros MD, de Melo Alves Da Silva VM and de Menezes Lima VL (2023). Antioxidant, anti-inflammatory and analgesic activity of *Mimosa acutistipula* (Mart.) Benth. *J. Ethnopharmacol*., **303**: 115964.

Cheung K, West G and Das DB (2015). Delivery of large molecular protein using flat and short microneedles prepared using focused ion beam (FIB) as a skin ablation tool. *Drug Deliv. Transl. Res*., **5**(4): 462-467.

Deodhar A, Maculaitis MC, Kopenhafer L, Beusterien K, Ling Y, Hauber B, Cappelleri JC, Yndestad A, Phillips LR and Zayed M (2026). Patients' perspectives regarding ankylosing spondylitis treatment administration features: Evidence from qualitative interviews and a multinational quantitative preference survey. *Rheumatol. Ther*., **13**(2): 329-346.

Ghosh M, Dandekar AA, Banga AK and Puri A (2026). Advancing transdermal drug delivery: Integration of microneedle technology and iontophoresis for enhanced therapeutic outcomes. *Expert Opin. Drug Deliv*., **23**(8): 1511-1530.

Gupta J, Gupta R and Vanshita (2021). Microneedle technology: An insight into recent advancements and future trends in drug and vaccine delivery. *Assay Drug Dev. Techn.*, **19**(2): 97-114.

Hu R, Yao B, Geng Y, Zhou S, Li M, Zhong W, Sun F, Zhao H, Wang J, Ge J, Wei R, Liu T, Jin J, Xu J and Fu J (2024). High-fidelity bioelectrodes with bidirectional ion-electron transduction capability by integrating multiple charge-transfer processes. *Adv. Mater.*, **36**(35): 2403111.

Huang W, Ling S, Li C, Omenetto FG and Kaplan DL (2018). Silkworm silk-based materials and devices generated using bio-nanotechnology. *Chem. Soc. Rev.*, **47**(17): 6486-6504.

Jiang H, Zhang X, Li X, Li Y, Yang X, Lv Y, Song W, Tian W and Xu B (2026). Electrically modulated semi-convertible hydrogel microneedles for programmable insulin delivery. *Adv. Mater.*, **38**(36): e73455.

Kovacik A, Kopecna M and Vavrova K (2020). Permeation enhancers in transdermal drug delivery: Benefits and limitations. *Expert Opin. Drug Deliv*., **17**(2): 145-155.

Lantz L, Holmes K and Douagi I (2023). Conjugation of fluorochromes to monoclonal antibodies. *Current Protocols*, **3**(6): e795.

Larrañeta E, Moore J, Vicente-Pérez EM, González-Vázquez P, Lutton R, Woolfson AD and Donnelly RF (2014). A proposed model membrane and test method for microneedle insertion studies. *Int. J. Pharm.*, **472**(1-2): 65-73.

Li AB, Kluge JA, Guziewicz NA, Omenetto FG and Kaplan DL (2015). Silk-based stabilization of biomacromolecules. *J. Control. Release*, **219**: 416-430.

Li X, Chen Y, Shao H, Yan Z, Wang Y and Lu S (2025).

Article in Press

Silk fibroin microneedles loaded with melatonin for circadian rhythm regulation. *Int. J. Biol. Macromol.*, **301**: 140500.

Lin Y, Zhao L, Jin H, Gu Q, Lei L, Fang C and Pan X (2025). Multifunctional applications of silk fibroin in biomedical engineering: A comprehensive review on innovations and impact. *Int. J. Biol. Macromol.*, **309**: 143067.

Liu Y, Li X, Ge L and Zhang Z (2024). Ultralarge-area stitchless scanning probe lithography and in situ characterization system using a compliant nanomanipulator. *Ieee-Asme Trans. Mechatron.*, **29**(2): 924-935.

Lu X, Sun Y, Han M, Chen D, Wang A and Sun K (2022). Silk fibroin double-layer microneedles for the encapsulation and controlled release of triptorelin. *Int. J. Pharm.*, **613**: 121433.

Mao Q, Ruan J, Cai X, Lu W, Ye J, Yang J, Yang Y, Sun X, Cao J and Cao P (2013). Antinociceptive effects of analgesic-antitumor peptide (AGAP), a neurotoxin from the scorpion Buthus martensii Karsch, on formalin-induced inflammatory pain through a mitogen-activated protein kinases-dependent mechanism in mice. *PLoS One*, **8**(11): e78239.

Meng S, Zhang C, Shi W, Zhang X, Liu D, Wang P, Li J and Jin Y (2016). Preparation of osthole-loaded nano-vesicles for skin delivery: Characterization, *in-vitro* skin permeation and preliminary *in-vivo* pharmacokinetic studies. *Eur. J. Pharm. Sci.*, **92**: 49-54.

Moawad F, Pouliot R and Brambilla D (2025). Dissolving microneedles in transdermal drug delivery: A critical analysis of limitations and translation challenges. *J. Control Release*, **383**: 113794.

Mosaddeghi-Heris R, Pandeh M, Ghorbi L, Taheri N, Shariat Zadeh M, Bagheri K and Martelletti P (2026). Stinging salvation: Harnessing scorpion venom peptides for revolutionary pain relief. *Toxins*, **18**(3): 120.

Ng FL, Cen Z, Toh Y and Tan LP (2024). A 3D - printed micro-perfused culture device with embedded 3D fibrous scaffold for enhanced biomimicry. *Int. J. Bioprinting*, **10**(1): 0026.

Oshizaka T, Hayakawa M, Uesaka M, Yoshizawa K, Kamei T, Takeuchi I, Mori K, Itakura S, Todo H and Sugibayashi K (2023). Design of an ante-enhancer with an azone-mimic structure using ionic liquid. *Pharm. Res.*, **40**(6): 1577-1586.

Qi Z, Tao X, Tan G, Tian B, Zhang L, Kundu SC and Lu S (2023). Electro-responsive silk fibroin microneedles for controlled release of insulin. *Int. J. Biol. Macromol.*, **242**: 124684.

Saeidi Z, Giti R, Rostami M and Mohammadi F (2023). Nanotechnology-based drug delivery systems in the transdermal treatment of melanoma. *Adv. Pharm. Bull.*, **13**(4): 646-662.

Su J, Yang Q, Zhang N, Zhou S, Li R, Hou S, Ge X, Zhou T, Zhang H, Dai Z and Wang J (2025). Synergistic effects of thermally induced gradient wettability and pore structure in thermoresponsive polymer-functionalized polyester knitted fabrics for adaptive thermal and moisture regulation. *ACS Appl. Mater. Interfaces*, **17**(47): 64992-65005.

Tan JM, Reeve E, Fraser L, Proudman SM and Wiese MD (2023). Barriers and enablers in the use of parenteral methotrexate in rheumatoid arthritis patients: A scoping review. *Arthritis Care Res.*, **75**(11): 2306-2315.

Van Damme P, Oosterhuis-Kafeja F, Van der Wielen M, Almagor Y, Sharon O and Levin Y (2009). Safety and efficacy of a novel microneedle device for dose sparing intradermal influenza vaccination in healthy adults. *Vaccine*, **27**(3): 454-459.

Wang H, Tang C, Zhang H, Guo L, Zou C, Zhang S, Liu J, Huang Q, Liu Y, Zhou W, Yang G and Gao X (2025). A biocompatible tea polyphenol nanoplatform for efficient cytosolic delivery of protein therapeutics. *J. Control. Release*, **388**: 114347.

Wang H, Zhang Y, Zhang M and Zhang Y (2024). Functional modification of silk fibroin from silkworms and its application to medical biomaterials: A review. *Int. J. Biol. Macromol.*, **259**: 129099.

Wang Y, Xu Y, Zhai W, Zhang Z, Liu Y, Cheng S and Zhang H (2022). In-situ growth of robust superlubricated nano-skin on electrospun nanofibers for post-operative adhesion prevention. *Nat. Commun.*, **13**(1): 5056.

Wei Q, He Z, Li Z, Zhou Z, Piao Y, Huang J, Geng Y, Zhang R, Fu Y, Ye J, Yuan Y, Zhu H, Zeng J, Zhang Y, Zhou Q, Xu M, Shao S, Tang J, Xiang J, Chen R, Zhou R and Shen Y (2025). A skin-permeable polymer for non-invasive transdermal insulin delivery. *Nature*, **648**(8093): 459-467.

Wu C, Yu Q, Huang C, Li F, Zhang L and Zhu D (2024). Microneedles as transdermal drug delivery system for enhancing skin disease treatment. *Acta Pharm Sin. B*, **14**(12): 5161-5180.

Xiao L, Gong H, Tan X, Chen P, Yang Y, Zhu H and Zhong S (2025). Physicochemical characterization and antitumor activity *in-vitro* of a polysaccharide from Christia vespertilionis. *Int. J. Biol. Macromol.*, **290**: 139095.

Yang J, Zhu J, Lu S, Qin H and Zhou W (2025). Transdermal psoriasis treatment inspired by tumor microenvironment-mediated immunomodulation and advanced by exosomal engineering. *J. Control. Release*, **382**: 113664.

Yin Z, Kuang D, Wang S, Zheng Z, Yadavalli VK and Lu S (2018). Swellable silk fibroin microneedles for transdermal drug delivery. *Int. J. Biol. Macromol.*, **106**: 48-56.

Zeng H, Zhang Y, Zhang M, Liu H, Liu J, Zhu L, Wang J and Guo W (2025). A signal enhanced lateral flow immunoassay based on core - shell quantum dots labeled antibody and antigen for sensitive detection of CP4-EPSPS protein. *Microchem J.*, **209**: 7.

Zhang W, Jiao Y, Zhang Z, Zhang Y, Yu J and Gu Z

Article in Press

(2024). Transdermal gene delivery. *J. Control. Release*, **371**: 516-529.

Zheng Y, Cheng H, Jiang S and Tai W (2025). Fc multisite conjugation and prolonged delivery of the folate-targeted drug conjugate EC140. *Bioconjug. Chem.*, **36**(4): 762-769.

Zhu M, Liu Y, Jiang F, Cao J, Kundu SC and Lu S (2020). Combined silk fibroin microneedles for insulin delivery. *ACS Biomater. Sci. Eng.*, **6**(6): 3422-3429.

Zhu T, Yu X, Yi X, Guo X, Li L, Hao Y and Wang W (2022). Lidocaine-loaded hyaluronic acid adhesive microneedle patch for oral mucosal topical anesthesia. *Pharmaceutics*, **14**(4): 15.

Article in Press